ELASTIC ELECTRON SCATTERING ON ^{4}He AT ENERGIES BETWEEN 30 AND 59 MeV

U. Erich, H. Frank, D. Haas and H. Prange

Institut für Technische Kernphysik der Technischen
Hochschule Darmstadt

Zeitschrift für Physik 209, 208-218 (1968)

Translated at CERN by H. MacCabe
(Original: German)
Not revised by the Translation Service

(CERN Trans. 71-13)

Geneva

March 1971

ELASTIC ELECTRON SCATTERING ON ^4He AT ENERGIES BETWEEN 30 AND 59 MeV

U. Erich, H. Frank, D. Haas*) and H. Prange

Institut für Technische Kernphysik der Technischen
Hochschule Darmstadt

Zeitschrift für Physik 209, 208-218 (1968)

*) Now at the Institut für Experimentalphysik der Ruhr-Universität, Bochum.

The cross section of ^{4}He for elastic electron scattering has been measured relative to that of the proton using a gas target with helium, hydrogen or a mixture of both gases. Scattering angles were between 56° and 130°, and the energy varied from 30 to 59 MeV. A model independent r.m.s. charge radius of (1.63 ± 0.04) fm has been evaluated for the α-particle.

I. INTRODUCTION

Measurements of the elastic electron scattering cross section at comparatively low momentum transfers q are used to determine the r.m.s. radius $R_m = \langle r^2 \rangle^{\frac{1}{2}}$ of the nuclear charge distribution. So far, measurements of the form factor F of the α-particle have been made at high momentum transfers (see References 1 to 7); they can be used to derive a charge distribution and hence to calculate R_m. The determination of R_m, on the other hand, is equivalent to a statement regarding dF/dq^2 for $q^2 \rightarrow 0$. The data communicated below will extend the experiments carried out to date to low momentum transfers, allowing R_m to be indicated independently of model assumptions.

We have used a gas target and have examined helium in relation to hydrogen. Except for the effects connected with the diverse recoil energies, the scattering on ^{4}He and ^{1}H has been observed under identical conditions. The recoil variations also allow measurements to be made with mixtures of gases, making it possible to eliminate, for instance, time-dependent changes of the entire assembly to a large extent. Using the known values of σ_p (for the sake of simplicity, σ will henceforth be used to designate $d\sigma/d\Omega$), the scattering cross section σ_α is determined from the experimentally obtained cross section ratios σ_α / σ_p. $R_m(\alpha)$ is then derived from the differences between this cross section and that for a point nucleus. However, these differences are so small within the examined q-range that, in evaluating the form factor, allowance must also be made for the small differences between the first Born approximation and an exact calculation despite the atomic number $Z = 2$.

The reference cross section σ_p has been calculated with the Rosenbluth formula, using form factors obtained from previous publications. However, owing to the smallness of the proton radius, the uncertainties with respect to the latter reflect only to a small extent on the radius of the α-particle as determined by us.

A brief review of the first results has already been published (see Reference 8). The accuracy of the measurements has meanwhile been increased by the use of a gas target cooled to 90° K and possessing a higher density. In addition, an improved procedure has been applied to the partial wave calculations (see foot-notes 9 to 11) and the systematic error sources have been examined in greater detail.

2. EXPERIMENTAL ASSEMBLY

The basic measuring procedure is shown in the diagram in Figure 1. Behind the analysing system, the electron beam from the Darmstadt linear accelerator (see Reference 12) is focussed onto the centre of the scattering chamber (beam diameter < 3 mm), which contains a thin-walled pressure vessel as the target. The unscattered electrons go into a beam trap. The charge collected there serves to measure the number of incident target electrons. It is expressed by the counting rate. Multiple scattering prevents a small number of electrons from being caught in the beam trap, but since, in practice, only the target wall produces this effect, the resulting loss is independent of the gas filling. The electrons which have been scattered at an angle θ in the gas enter a double-focusing magnetic spectrometer of 120°. Electrons which are scattered at the target walls cannot reach the spectrometer directly, but they produce, through double or multiple scattering, a background which can be measured when the target is empty and which is significantly reduced by the diaphragm installed between the target and the spectrometer.

For sixteen measurements, a coincidence assembly consisting of two plastic scintillators behind a tungsten diaphragm served as detector (see Reference 12). Afterwards, fourteen measurements were made with a non-coincidence five-channel detector consisting of five closely placed plastic scintillators (11 x 11 x 1 mm^3). Owing to the recoil, the hydrogen and the helium lines are 3.9 MeV apart at the highest momentum transfer. An energy-dependent counter yield probability would have necessitated a correction of the experimental values, but test measurements have shown that this effect accounts for less than 0.3% in σ. This uncertainty has also been taken into account in the evaluation of the error of R_m.

Figure 2 shows a target assembly for measurements at the temperature of liquid nitrogen. There was no background increase compared with the targets not subjected to cooling (without cooling vessel), but, at the same pressure, the gas density is considerably higher. Whereas the determination of σ_α / σ_p at room temperature included also individual measurements (precision of pressure measurement : 0.3%), only mixtures were used at low temperatures. The density ratio of the two gases was ascertained with a mercury pressure gauge to an accuracy of 0.2% at room temperature and under low pressure at the time when the mixture was produced. After the two components had been carefully mixed, the gas was brought up to the working pressure in the target (approximately 10 kp/cm^2) by means of a Toepler pump. With a filled and cooled target, the temperature increase of the target wall (obtained with Au/Co-Fe thermocouples) amounted to approximately 2° for a beam current of 1 μA (about 80° for the evacuated target). Since the volume of the gas in the target was closed off, the density of the gas was not affected by the change in temperature.

3. MEASUREMENT AND EVALUATION

Figure 3 shows a typical spectrum, obtained with a mixture of helium and hydrogen at 90°K. It indicates the "counting rate" ζ (i.e. the number of pulses in relation to the charge collected in the beam trap) as a function of the electron energy. The points given by the experiment were corrected for the dead time losses of the counters ($<$ 1%). Two lines are apparent; compared with the pre-scattering energy E_0 they show a shift amounting to the relevant recoil energy. The line widths are determined by the form of the primary spectrum, the energy resolution of the spectrometer, the energy loss and scattering at the target walls, and the finite solid angle (recoil energy variation with Θ). In the example of Figure 3, the last effect is dominant and the H-line is thus wider than the He-line. In order to evaluate the areas z_i below the lines ζ_i (equation 1b), the background, obtained with the evacuated target, was first deducted from ζ. To the right of the He-line, the background was the same with and without the gas filling; hence, the scattering within the gas does not produce any measurable additional background. Another measurement with helium alone allowed the portion of the helium line below the hydrogen line to be obtained.

The connection between σ ($\equiv d\sigma/d\Omega$) and the experimental values is given by

$$\sigma_\alpha/\sigma_p = (z_\alpha/z_p) \cdot (N_p/N_\alpha) \cdot (K_p/K_\alpha) \qquad (1a)$$

where

$$z_i = \int_a^b \zeta_i \, dE/E. \qquad (1b)$$

The index indicates the scattering nucleus. The ratio of the target nuclei per volume N_p/N_α was calculated from the pressure ratio, allowance being made for the virial coefficients for real gases. The factor $1/E$ in the line integral in equation (1b) takes the dispersion of the spectrometer into account. The choice of the upper integration limit b is not a problem, because the counting rate drops to the background. In view of the extension at low energies (radiation tail), however, the cut-off at the lower limit a calls for a correction K. In a gas target, the corrections for the bremsstrahlung and energy loss distribution are determined by the target wall; for He and H, the coincidence is better than 0.1%. Accordingly, K_p/K_α is from now on assumed to equal the ratio of the radiative corrections and has been calculated in accordance with the formula indicated by TSAI (see Reference 14, with Z = 1 for H and Z = 2 for He in equation III,22). For the purpose of introducing the cut-off energy $E_\alpha - a = \Delta E$ into K_α, E_α was assumed to be the center of the half-width of the line. The same ΔE was also chosen for the proton; it amounted to two to three half-widths of the lines. A ΔE-dependence of the ratio σ_α / σ_p, evaluated in accordance with equation (1a), could not be established within this range.

With the calibration of the spectrometer known to an accuracy of 0.1% (see Reference 12), the mean electron energy E_o in the laboratory system prior to scattering was obtained from the position of the lines E_α resp. E_p, and correction was made for the energy loss in the target wall and in the gas. The uncertainty of E_o amounted to less than 0.2%.

The cross sections in equation (1) should be averages over the finite solid angle defined by the diaphragms and the multiple scattering in the target wall. No account was taken of this fact because, with the scattering angles examined here, the use of the averages would have changed the ratio $\sigma_\alpha / \sigma_\rho$ in equation (1a) by less than 0.1%.

The cross section σ_ρ was calculated with the Rosenbluth formula

$$\sigma_p = \sigma_0 [(G_E^2 + \tau^2 G_M^2)/(1+\tau^2) + 2\tau^2 G_M^2 \cdot \mathrm{tg}^2(\Theta/2)]$$
$$\tau = \hbar q_p / 2M_p c; \quad \hbar^2 q_p^2 = (\vec{p}_1 - \vec{p}_2)^2 - (E_1 - E_2)^2/c^2 \qquad \text{(2a)}$$
$$\sigma_0 = \sigma_M / \eta_p \qquad \text{(see equation (6)).}$$

In the above, $G_E(q_p)$ and $G_M(q_p)$ are the form factors for the charge resp. magnetic moment distribution of the proton; their dependence on the momentum transfer q_p is obtained from the results of high energy electron scattering. As the contribution of the terms involving G_M is small in the examined angular range, any difference between G_E and $G_M/2.793$ can be ignored; a good fit is obtained with the assumption that $G_E = G_M/2.793 = G$ (see Reference 15). For R_p=0.80 fm, this form factor was calculated according to HOFSTADTER [following a private communication (mean for Landolt-Börnstein) as per Reference 16] in the approximation

$$G = 1 - R_p^2 q_p^2/6 + R_p^4 q_p^4/48, \qquad (2b)$$

the contribution of the higher terms of the charge distribution (which is small for $q_p^2 < 0.3$ fm^{-2}) being accounted for by the second term of the series expansion for the form factor of an exponential charge distribution (see References 16, 17). In equation (2a), σ_0 equals the Mott cross section for a point nucleus without spin, multiplied by the recoil term $1/\eta$ (as in equation (6)).

Table 1 shows the results of all the measurements. They are listed according to the values of q^2 and marked to show the experimental conditions, i.e. whether He and H_2 were examined individually one after the other (E) or simultaneously in a mixture (M), whether the measurements were made at low temperature (x) or at room temperature (y), and what detector system (v or w) was used. The other letters indicate the scattering angles of the spectrometer settings.

Equation (2) allows σ_α to be calculated from the experimental values σ_α / σ_p. The relative error of σ_α / σ_p is equal to the error $\Delta F^2/F^2$ set out in the last column. It consists of the errors of N_p/N_α and z_α / z_p; the inaccuracy of the area determination z_i (which results from the counting statistic and from uncertainties due to small energy changes during measurement) is predominant. Through σ_p , the cross section σ_α is also affected by the energy error. However, for $\Delta E/E \leq 0.2\%$, the term $\Delta \sigma_\alpha / \sigma_\alpha$ is, in practice, also equal to the figures in the last column.

4. RADIUS OF THE α-PARTICLE

$R_m(\alpha)$ can be obtained from the experimental cross sections σ_α by a fit with theoretically determined cross sections. Since, for $Z = 2$, the first Born approximation differs little from the exact calculation, this difference was calculated for a nucleus with $Z=2$, using a Gaussian function for the charge distribution and $R_m = 1.63$ fm (*), so as to add it, for the evaluation of σ_α, as a correction $\varepsilon\ (\Theta, E)$ to the first Born approximation. In this way, it has been possible to derive the form factor (**) from the experimentally obtained cross section.

BÜHRING's Programme (see References 9 to 11) was used for the calculation with the partial wave method, the correction being calculated according to equation (3)

$$\sigma_s = \sigma_M \cdot F^2(q)\left(1 + \varepsilon(\Theta_s, E_s)\right) \qquad \text{(3a)}$$

(*) ε being small, the difference between this preselected radius and the radius obtained in the evaluation can be neglected here, being a higher order correction.

(**) defined as Fourier transform of the charge distribution.

with the Mott cross section

$$\sigma_M = \left(\frac{Ze^2}{2E_s}\right)^2 \cdot \frac{1-\beta^2 \sin^2(\Theta_s/2)}{\beta^4 \sin^4(\Theta_s/2)} \quad . \qquad \text{(3b)}$$

Here, the first terms of the series expansion

$$F(q) = 1 - \tfrac{1}{6}\langle r^2\rangle q^2 + \tfrac{1}{120}\langle r^4\rangle q^4 - + \cdots \qquad \text{(4)}$$

provide a sufficient degree of accuracy for the form factor.

The index s indicates the center-of-mass system (*); values without indices relate to the laboratory system. The Lorentz-invariant four momentum transfer q is obtained from

$$q = \frac{2E_s}{\hbar c} \cdot \sin\frac{\Theta_s}{2} = \frac{2E}{\hbar c} \cdot \frac{\sin(\Theta/2)}{\sqrt{\eta}} \qquad \text{(5a)}$$

where

$$\eta = 1 + (1-\cos\Theta)\, E/Mc^2. \qquad \text{(5b)}$$

The conversion of the cross section from the center-of-mass system to the laboratory system gives

$$\sigma(\Theta, E) = \eta^{-1}\sigma_M(\Theta, E)\, F^2(q)\left(1 + \varepsilon(\Theta_s, E_s)\right), \qquad \text{(6)}$$

(*) The cross sections calculated for a nucleus with infinite mass have been put equal to the required cross sections in the center-of-mass system.

if, in σ_M (see equation (3b)), Θ_s and E_s are replaced by the laboratory system values Θ and E. E_s and Θ_s were derived from E resp. Θ according to DEDRICK (see Reference 18). The second powers of the form factors, obtained from σ_α by means of equation (6), are set out in Table 1 together with their errors.

The form factor thus derived should only depend on q^2 (and not individually on E and Θ) (see, for instance, Figure 4). In particular, the experimental values should permit an extrapolation to F=1 for $q^2=0$. In evaluating $R_m(\alpha)$ by applying a least squares fit to equation (4), account was also taken of the small contribution of the higher terms of the charge distribution in F, a Gaussian function being assumed. In order to test for systematic errors, a fit was also made to a function with a free scale factor B :

$$F^2 = B \exp\left(-R_m^2 q^2/3\right). \qquad (7)$$

The results are set out in lines 3 and 4 of Table 2.

Another correction suggests itself; it concerns the proton cross section and takes account of the difference we must expect between the true cross section and the Rosenbluth formula in the first Born approximation. In analogy to the calculation made for the α-particle, a correction $\varepsilon_p(\Theta,E)$ was computed, using the partial wave method, for a nucleus without spin for $Z = 1$ and $R_p = 0.8$ fm. It amounts to approximately 1% and is included in Table 1 in order to allow an easy conversion of σ_α and F^2 by multiplying with $(1+\varepsilon_p)$. The result of the evaluation with this correction (for ε_p, see Table 1) is shown in the first two lines of Table 2.

Both for $\varepsilon_p \neq 0$ (first line) and for $\varepsilon_p = 0$ (third line), the value for the free scale factor B is compatible with $B = 1$ within the statistical errors. Thus, both evaluations, taken individually did not indicate any systematic errors, so that an evaluation using a given fixed $B = 1$ might seem justified. However, the differences in the ordinate sections show how systematic scale errors can be introduced by the choice of the evaluation. If, therefore, the difference B-1 is assumed to be the most probable scale error in each case, and if R_m is evaluated on the basis of the fit without the constraint $F^2=1$ for $q=0$, the result, compared with the $B=1$ evaluation, shows little variance. For the purpose of comparison, the result of the first Born approximation is shown in lines 5 and 6. Here, the difference between B and $B=1$ is more than twice the statistical error, whereas, for a preselected fixed $B=1$, a considerably larger value of χ^2 is found than for all other fits. The fact that the R_m differences are small for a free B (first, third and fifth lines) is explained by the small variation of the ε- corrections with q within the considered angular range.

Figure 4 shows the form factors obtained with $\varepsilon_p = 0$ and $\varepsilon_\alpha \neq 0$. The experimental values for identical momentum transfers have been combined in a mean value with a correspondingly reduced error. In one instance ($q^2 = 0.109\ \mathrm{fm}^{-2}$), the figure shows, in addition, the angular distribution of the relevant experimental values. Within the measuring errors, the expected independence of Θ exists. The ~~uninterrupted~~ solid curve corresponds to equation (7) with B=1, the ~~interrupted~~ dashed straight line takes only account of the term containing $\langle r^2 \rangle$ in equation (4). Both curves have been calculated with $R_m = 1.64$ fm. The figure shows the small influence of the term containing $\langle r^4 \rangle$ in equation (4), hence the independence from special model assumptions.

We must still consider the fact that we have used form factors for σ_p which have been derived from a fit of the Rosenbluth formula (without corrections) to high energy measurements. Therefore, a somewhat smaller ε_p should probably be chosen than indicated in Table 1 or, conversely, a somewhat larger R_p should be assumed. ε_p being small for the form factors obtained at high energies, the change to be expected in R_p should be smaller than the errors indicated by HOFSTADTER ($R_p = 0.80 \pm 0.02$ fm) (see foot-note 16) and has therefore not been taken into consideration here.

In accordance with line 1 of Table 2, we indicate

$$R_m = \langle r^2 \rangle^{\frac{1}{2}} = (1{,}63 \pm 0{,}04)\ \mathrm{fm}$$

as the current result for the r.m.s. charge radius of the α-particle. The error takes account of the uncertainty applying to the proton radius and to the counter yield probability (Chapter 2); it further includes the values obtained by the other evaluations (lines 2 to 4).

Our value for R_m should be compared with the following published values : (1.60 0.1)fm (see Reference 2),

(1.68 0.04)fm (see References 4 and 7),

1.71 fm (see Reference 7),

a Gaussian function for the charge distribution having been assumed for the first two values, a Fermi function with 3 parameters for the last. Since these values are based on measurements of high momentum transfers, R_m varies with the chosen charge distribution model (see, for instance, References 6 and 7 for other data concerning the radius and Reference 5 for other form factor fits which give 1.49 fm $\leqq R_m \leqq$ 1.60fm). The radius indicated by us is free from such an uncertainty.

The experiments are being continued with the aim of reducing both the experimental errors and the uncertainties in the evaluation.

In addition, a re-examination of the theory of radiation corrections could, at the accuracy required here, influence the calculation of the radius.

To Professor Dr. P. Brix, who suggested the work, we wish to express our particular gratitude for many productive discussions. We are indebted to Dr. R. Engfer, Dr. W. Bühring and H.A. Bentz for the computing programmes placed at our disposal and for their valuable support, to Dr. A. Körding for his critical examination of the manuscript and to H. Schnitger and K.J. Böttcher for their help with the experiments. Work done by the entire DALINAC Group furnished essential experimental prerequisites and we take this opportunity to extend to them our cordial thanks.

This work was sponsored by the Bundesministerium für wissenschaftliche Forschung.

REFERENCES

1) R. Hofstadter, Rev. Mod. Phys. 28, 214 (1956).

2) R.W. McAllister and R. Hofstadter, Phys. Rev. 102, 851 (1956).

3) R. Blankenbecler and R. Hofstadter, Bull. Am. Phys. Soc. 1, 10, AB6 (1956).

4) G.R. Burleson and H.W. Kendall, Nuclear Phys. 19, 68 (1960).

5) J.P. Repellin, P. Lehmann, J. Lefrançois and D.B. Isabelle, Phys. Letters 16, 169 (1965).

6) R.F. Frosch, R.E. Rand, K.J. van Oostrum and M.R. Yearian, Phys. Letters 21, 598 (1966).

7) R.F. Frosch, J.S. McCarthy, R.E. Rand and M.R. Yearian, Phys. Rev. 160, 874 (1967).

8) H. Frank, D. Haas and H. Prange, Phys. Letters 19, 391 (1965).

9) W. Bühring, Z. Physik 187, 180 (1965).

10) W. Bühring, Z. Physik 192, 13 (1966).

11) H.A. Bentz, R. Engfer and W. Bühring, Nuclear Phys. A101, 527 (1967).

12) F. Gudden, G. Fricke, H.G. Clerc and P. Brix, Z. Physik 181, 453 (1964).

13) M. Stroetzel, Laborbericht Nr. 19, Institut für Technische Kernphysik der T.H. Darmstadt (1965).

14) Tsai, Yung-Su, Phys. Rev. 122, 1898 (1961).

15) B. Dudelzak, Thèse, Orsay, Série A, No. 103 (1965).

16) R. Hofstadter, Private Mitteilung (Mittelwert für Landolt-Börnstein).

17) L.H. Chan, K.W. Chen, J.R. Dunning Jr., N.F. Ramsey, J.K. Walker and R. Wilson, Phys. Rev. 141, 1928 (1966).

T. Janssens, R. Hofstadter, E.B. Hughes and M.R. Yearian, Phys. Rev. 142, 922 (1966).

18) K.G. Dedrick, Rev. Mod. Phys. 34, 429 (1962).

Table 1 : Parameters and Experimental Results

q^2 [fm^{-2}]	E_0 [MeV]		K_p/K_α	ΔE [keV]	σ_α/σ_p	σ_α [fm^2/sr]	ε_α [%]	ε_p [%]	F^2	$\Delta F^2/F^2$ [%]
0,02026	29,59	*a,y,w,E*	1,0038	311	4,042	$3{,}568\cdot10^{-2}$	1,48	0,77	0,9835	1,3
0,02026	29,59	*a,y,w,M*	1,0038	311	4,049	$3{,}574\cdot10^{-2}$	1,48	0,77	0,9853	1,4
0,03953	34,81	*b,y,w,E*	1,0041	349	3,947	$1{,}097\cdot10^{-2}$	1,60	0,85	0,9521	1,2
0,03953	34,81	*b,y,w,M*	1,0041	346	4,048	$1{,}126\cdot10^{-2}$	1,60	0,85	0,9766	1,3
0,04859	30,13	*d,y,w,E*	1,0045	304	4,014	$3{,}822\cdot10^{-3}$	1,86	0,98	0,9636	1,3
0,04868	30,16	*d,y,w,E*	1,0045	323	3,947	$3{,}749\cdot10^{-3}$	1,86	0,98	0,9564	1,0
0,06678	35,35	*d,y,v,E*	1,0047	528	3,950	$2{,}718\cdot10^{-3}$	1,80	0,97	0,9454	1,5
0,06754	39,69	*c,y,v,E*	1,0045	436	3,834	$3{,}945\cdot10^{-3}$	1,70	0,92	0,9173	1,5
0,10858	36,30	*g,x,w,M*	1,0055	341	3,625	$3{,}977\cdot10^{-4}$	1,95	1,08	0,9028	1,0
0,10898	45,22	*d,x,w,M*	1,0051	405	3,863	$1{,}610\cdot10^{-3}$	1,69	0,96	0,9201	1,0
0,10916	57,96	*b,x,w,M*	1,0048	536	3,760	$3{,}699\cdot10^{-3}$	1,42	0,83	0,8950	1,0
0,10940	38,55	*f,y,v,E*	1,0054	520	3,652	$6{,}398\cdot10^{-4}$	1,88	1,05	0,8863	1,5
0,10940	38,55	*f,y,v,E*	1,0054	480	3,728	$6{,}532\cdot10^{-4}$	1,88	1,05	0,9049	1,5
0,12668	44,60	*e,y,v,M*	1,0054	532	3,715	$8{,}705\cdot10^{-4}$	1,75	1,00	0,8897	1,5
0,12668	44,60	*e,y,v,E*	1,0054	532	3,718	$8{,}712\cdot10^{-4}$	1,75	1,00	0,8905	1,5
0,12805	54,74	*c,y,v,M*	1,0051	622	3,772	$2{,}027\cdot10^{-3}$	1,53	0,90	0,8945	1,5
0,12805	54,74	*c,y,v,E*	1,0051	622	3,734	$2{,}006\cdot10^{-3}$	1,53	0,90	0,8855	1,5
0,13307	50,00	*d,y,w,E*	1,0053	413	3,674	$1{,}247\cdot10^{-3}$	1,64	0,95	0,8731	1,5
0,13317	50,02	*d,y,w,E*	1,0054	449	3,737	$1{,}268\cdot10^{-3}$	1,64	0,95	0,8881	1,2
0,19006	54,72	*e,y,v,E*	1,0060	646	3,534	$5{,}474\cdot10^{-4}$	1,60	0,98	0,8464	1,5
0,19006	54,72	*e,y,v,E*	1,0060	646	3,475	$5{,}383\cdot10^{-4}$	1,60	0,98	0,8323	1,5
0,19026	54,75	*e,y,v,E*	1,0060	646	3,443	$5{,}328\cdot10^{-4}$	1,60	0,98	0,8245	1,5
0,19047	54,78	*e,y,v,E*	1,0060	646	3,538	$5{,}469\cdot10^{-4}$	1,60	0,98	0,8473	1,5
0,19047	54,78	*e,y,v,E*	1,0060	646	3,427	$5{,}297\cdot10^{-4}$	1,60	0,98	0,8208	1,5
0,22504	55,47	*f,y,v,M*	1,0065	839	3,243	$2{,}758\cdot10^{-4}$	1,60	1,01	0,7986	1,5
0,22552	55,53	*f,y,v,M*	1,0065	614	3,387	$2{,}875\cdot10^{-4}$	1,60	1,01	0,8342	1,5
0,22552	55,53	*f,y,w,M*	1,0065	624	3,355	$2{,}848\cdot10^{-4}$	1,60	1,01	0,8263	1,5
0,27933	58,50	*g,x,w,M*	1,0072	471	2,892	$1{,}276\cdot10^{-4}$	1,53	1,02	0,7629	1,8
0,28103	58,68	*g,x,w,M*	1,0070	460	2,995	$1{,}315\cdot10^{-4}$	1,53	1,02	0,7905	1,6
0,28236	58,82	*g,y,v,M*	1,0071	426	2,992	$1{,}308\cdot10^{-4}$	1,52	1,02	0,7902	3,0

σ_α / σ_p are the values obtained from the experiments; they have been used to determine σ_α and F^2 for $\varepsilon_\alpha \neq 0$ and $\varepsilon_p = 0$.

The scattering angles are : a = 56.77°; b = 68.83°; c = 80.92°; d = 92.91°; e = 104.98°; f = 117.04°; g = 129.02°;

x = measurement at T=90° K; y = measurement at room temperature;

v = coincidence counters; w = 5-detector system; measurements made for He and H_2 in sequence (E) or simultaneously (M).

Table 2 : Results of the fit with χ^2-test

(f = number of degrees of freedom)

The errors cited here are statistical errors only.

	B	χ^2/f	R_m [fm]
$\varepsilon_\alpha \neq 0,\ \varepsilon_p \neq 0$	$1{,}0046 \pm 0{,}0051$	0,936	$1{,}63_3 \pm 0{,}034$
	1^a	0,931	$1{,}60_7 \pm 0{,}017$
$\varepsilon_\alpha \neq 0,\ \varepsilon_p = 0$	$0{,}9976 \pm 0{,}0051$	0,918	$1{,}64_7 \pm 0{,}034$
	1^a	0,896	$1{,}66_0 \pm 0{,}017$
$\varepsilon_\alpha = 0,\ \varepsilon_p = 0$	$1{,}0130 \pm 0{,}0051$	0,939	$1{,}64_3 \pm 0{,}034$
	1^a	1,128	$1{,}56_9 \pm 0{,}017$

a) assuming B = 1.

Figure 1 : Diagram of the Experimental Assembly

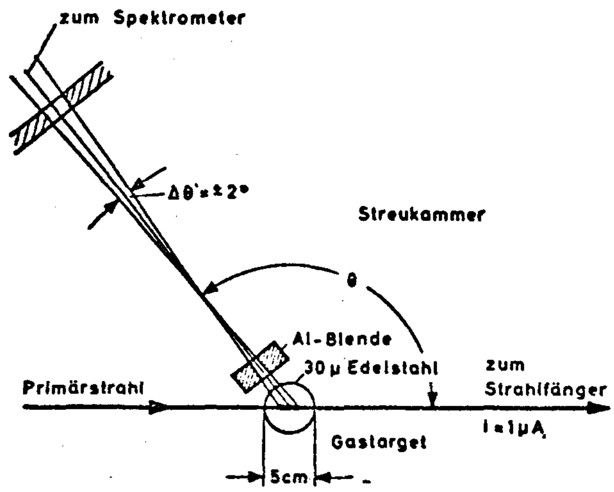

Legend: zum Spektrometer = to the spectrometer;
Streukammer = scattering chamber;
Primärstrahl = primary beam;
Al-Blende = Al diaphragm;
Edelstahl = tungsten steel;
Gastarget = gas target;
zum Strahlfänger = to the beam trap.

Figure 2 : Cooled gas target

(target cylinder shown in profile)

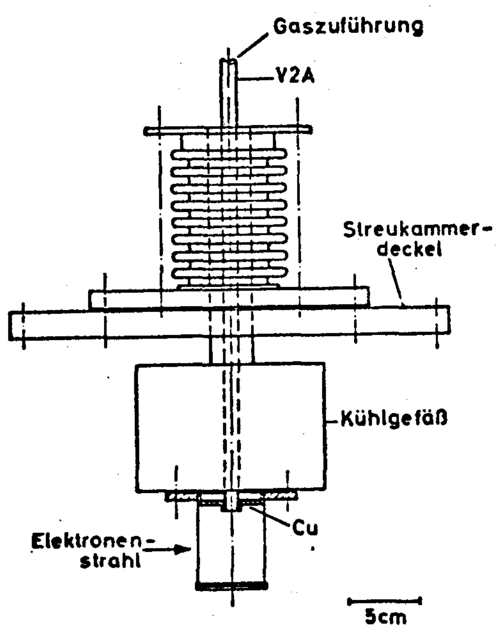

Legend : Gaszuführung = gas input;
Streukammerdeckel = lid of scattering chamber;
Kühlgefäss = cooling vessel;
Elektronenstrahl = electron beam.

Figure 3 : Electron scattering spectrum in a H_2/He mixture

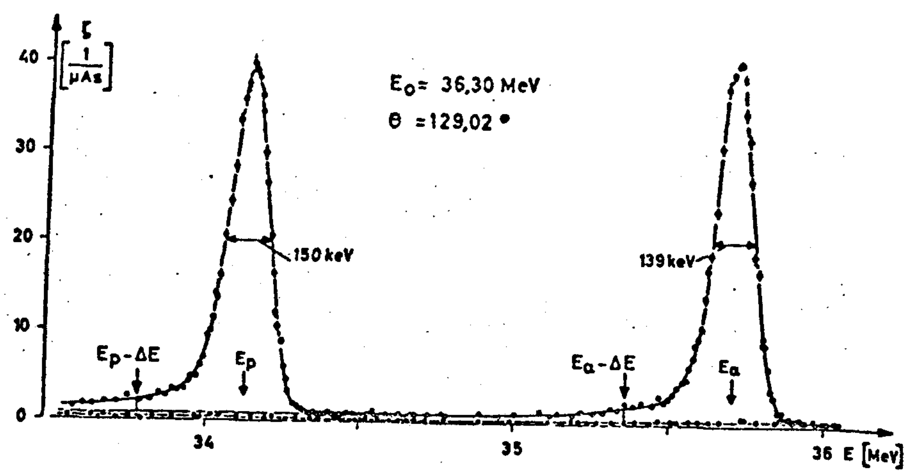

$T = 90^oK$, $p_{gas} = 9.45\ kp/cm^2$; $p(H_2)/p(He) = 1.911$;

Full circles : background ($\approx 0.4\ /\mu As$).

Below the H_2-line (at E_p), the separately established portion of the He-line is indicated.

Figure 4 : Form factor of the α-particle as a function of q^2

For the purposes of this Figure, the mean of the values indicated in Table 1 has been taken for each q^2.

Upper right : For $q^2 = 0.109\ \mathrm{fm}^{-2}$, the individual measurements are shown as a function of the angle (identical ordinate scale).

~~Uninterrupted~~ Solid curve : $F = \exp(-R_m^2 q^2/6)$

~~Interrupted~~ Dashed curve : $F = 1 - R_m^2 q^2/6$